

First minimum bias physics results at LHCb

Christian Linn, *on behalf of LHCb collaboration*
 Physikalisches Institut der Universität Heidelberg, Germany

The goal of the LHCb experiment is the indirect search for New Physics through precision measurements of B-decays. A short description of the detector and its performance after the first data taking in 2009 and 2010 will be presented. In addition first preliminary results of a K_s differential cross section measurement at a center of mass energy of $\sqrt{s} = 900$ GeV and a measurement of the $\frac{\lambda}{\bar{\lambda}}$ production ratio at $\sqrt{s} = 900$ GeV and $\sqrt{s} = 7$ TeV will be discussed.

1. Introduction

LHCb is a dedicated flavour-physics experiment to search for New Physics beyond the Standard Model through precision measurements of b hadron decays and CP violation. The large $b\bar{b}$ production cross section at the LHC leads to $\sim 10^{12}$ $b\bar{b}$ pairs per nominal operational (10^7 s) year at a luminosity of $2 \cdot 10^{32}$ $\text{cm}^{-2}\text{s}^{-1}$. The dominant production mechanism is through gluon-gluon fusion with asymmetric momenta of the incoming gluons. As a consequence the $b\bar{b}$ pair is strongly boosted either in forward or backward direction with respect to the pp center of mass system. Similar considerations hold for the production of charm mesons, with which many interesting measurements are also foreseen. Therefore the LHCb detector is designed as single arm forward spectrometer covering a pseudorapidity range $1.9 < \eta < 4.9$. Beside of the good acceptance for detecting b hadrons, this unique angular coverage gives the possibility for a wide field of forward minimum bias physics.

Hence, the first data collected in 2009 and 2010 at center of mass energies $\sqrt{s} = 900$ GeV and $\sqrt{s} = 7$ TeV were not only used to calibrate and understand the detector but also to obtain interesting forward physics results. At LHC especially strangeness production is an excellent test-field of hadronization and fragmentation models as there are no valence strange quarks in the initial state. So far there are several models available which disagree mainly in forward phase space regions. This makes the LHCb results to be a good probe of these models. As first LHCb measurements the differential K_s production cross section and the $\frac{\lambda}{\bar{\lambda}}$ production ratio will be presented here.

2. Detector description and performance

The aim of the LHCb detector to measure precisely the b hadrons and their decay products leads to specific detector requirements. An excellent vertex and proper time resolution is necessary to measure the fast oscillation of the B_s mesons. An efficient particle identification, especially for K/π separation, and an excellent momentum resolution for the precise invariant

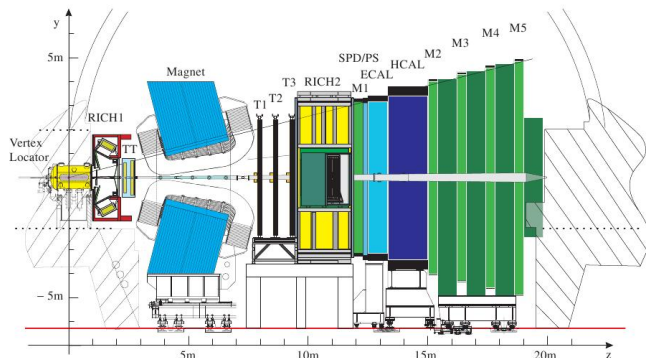


Figure 1: Side view of the LHCb detector showing the vertex locator (VELO), the Cherenkov detectors (RICH1, RICH2), the dipole magnet and the tracking stations (TT, T1-T3), the Scintillating Pad Detector (SPD), Preshower (PS), electromagnetic (ECAL) and hadronic (HCAL) calorimeters, and the five muon stations (M1-M5).

mass reconstruction is needed to reject background. The detector consists of a vertex locator (VELO), two Cherenkov detectors (RICH1-2) for particle identification, a tracking system with two stations before (TT) and three stations after (T1-3) a warm dipole magnet, electromagnetic (ECAL) and hadronic (HCAL) calorimeters and five muon stations (M1-5). A schematic layout of the detector is shown in Fig. 1. In the following a few detector components and their performance with the first LHC data are described in more detail. A complete description of the detector can be found in [1].

2.1. VELO and tracking system

The vertex locator is a silicon strip detector built of 21 stations positioned around the interaction region. The stations are made of half disks which measure the radial and azimuthal coordinates. The sensitive area of the sensors start at 8 mm from the beam axis. This small distance allows an excellent vertex resolution. Already in the first data a vertex resolution in the plane perpendicular to the beam axis of $\sim 15 \mu\text{m}$ was

achieved. To avoid damage when setting up the LHC beams the half disks can be retracted.

The spectrometer consists of a warm dipole magnet with an integrated magnetic field of ~ 4 Tm. Five tracking stations are used for a precise momentum measurement. The two stations before the magnet (TT) consist of four layers of silicon strip detectors. The three stations after the magnetic field are divided into two parts: the area close to the beam pipe (IT) covers most of the particle flux and is also made out of silicon strip detectors, whereas the outer part (OT) is constructed from drift straw tubes. The hit resolution of the silicon strip detectors determined with the first collision data is $\sim 60 \mu\text{m}$ for the TT and $\sim 55 \mu\text{m}$ for the IT. The straw tube detector has a hit resolution of $\sim 270 \mu\text{m}$, which is already close to the nominal value.

The expected momentum resolution of the tracking system, predicted from Monte Carlo, starts from $\frac{\delta p}{p} \sim 0.35\%$ for low momentum tracks and degrades for high momentum tracks up to $\frac{\delta p}{p} \sim 0.55\%$.

2.2. Particle identification

Ring imaging Cherenkov detectors (RICH) are used for particle identification. An efficient K/π separation is important for the necessary background rejection. The first RICH is located directly after the vertex locator. It uses C_4F_{10} gas and aerogel as radiators and covers a momentum range from 2 – 60 GeV. The second RICH using CF_4 as gas radiator is positioned after the tracking stations and extends the momentum coverage up to ~ 100 GeV. The average efficiency for kaon identification is $\epsilon(K \rightarrow K) \sim 95\%$ with a corresponding pion misidentification rate of $\epsilon(\pi \rightarrow K) \sim 5\%$. Electrons, photons and hadrons are identified with the calorimeter system, which is also used to measure their energies and positions. It is positioned after the RICH2 and consists of a scintillating pad detector, a preshower detector, the electromagnetic and hadronic calorimeter. The muon identification is done with the five muon stations, four of them located after the calorimeters. The muon identification efficiency $\epsilon(\mu) \sim 97\%$ was estimated from data and is in very good agreement with the Monte Carlo predictions.

3. K_s cross section measurement

The measurement of the differential K_s production cross section was done with the first data delivered by the LHC. In total 13 runs, taken in December 2009 with an integrated luminosity of $L = 6.8 \pm 1.0 \mu\text{b}^{-1}$ at a center of mass energy of $\sqrt{s} = 900$ GeV were used for this analysis. All detector components were in operation and the magnetic field was at nominal

strength. However, due to the low beam rigidity at lower energy the vertex detector halves were retracted 15 mm from their nominal position.

3.1. Analysis strategy

K_s mesons were reconstructed in the $\pi^+\pi^-$ mode using only events triggered by the calorimeters. Contributions from secondary interactions in the detector material or from the decay of long-lived particles were suppressed by requiring the K_s candidates to point back to the pp collision point. The analysis was performed in bins of transverse momentum p_T and rapidity $y = \frac{1}{2} \ln \frac{E+p_z}{E-p_z}$, calculated in the rest frame of the pp collision. The partial K_s cross section was calculated using $\sigma_{i,j} = \frac{N_{i,j}}{L \epsilon_{i,j}^{\text{trig}} \epsilon_{i,j}^{\text{reco}}}$ where $N_{i,j}$ is the observed signal yield in the respective (p_T, y) bin and $\epsilon_{i,j}^{\text{trig}}$ and $\epsilon_{i,j}^{\text{reco}}$ are the corresponding trigger and reconstruction efficiencies. The efficiencies were calculated from a fully simulated Monte Carlo sample of single pp collisions and checked with data. Details are described in [2]. No separation of K_s produced in diffractive and non-diffractive events was attempted.

3.2. Luminosity measurement

The integrated luminosity was determined using measurements of beam currents and the size of the colliding beam bunches. The luminosity produced by one pair of colliding bunches can be expressed as

$$L = f \sum \frac{n_1 n_2}{4\pi \sigma^x \sigma^y} \quad (1)$$

where n_1, n_2 are the numbers of protons in bunch 1 and 2, $f = 11.245\text{kHz}$ is the LHC revolution frequency and σ^x, σ^y are the bunch sizes in the transverse (x, y) plane. The beam sizes were reconstructed using tracks produced in beam-beam and beam-gas collisions in the VELO and the bunch currents are measured by the LHC machine team. This procedure has a systematic uncertainty $\sim 15\%$ which is dominated by the measurement of the beam currents delivered from the LHC machine.

3.3. Event selection

K_s candidates were reconstructed from any combination of two oppositely charged tracks, assumed to be pions. Due to the relatively long lifetime of the K_s and the open VELO position, most of the tracks have no VELO information. Therefore the K_s were selected using two different approaches:

The downstream-track selection uses tracks with hits in the tracking stations (TT and T1-T3) only, ignoring any VELO information. The selection is based on track quality cuts and requires the reconstructed K_s

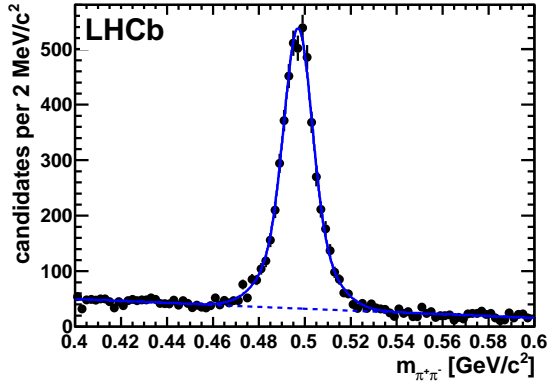


Figure 2: Mass distribution of all selected K_s candidates in the downstream-track analysis with the overlaying fit, described in the text.

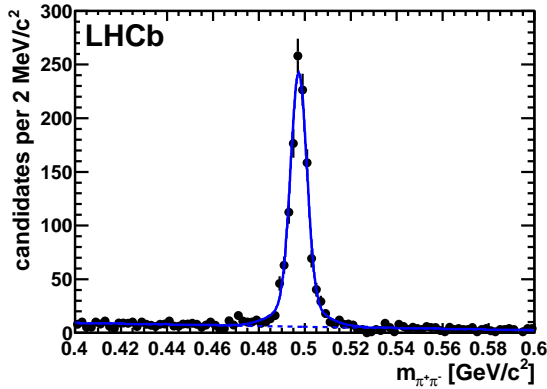


Figure 3: Mass distribution of all selected K_s candidates in the long-track analysis with the overlaying fit, described in the text.

to point back to the primary vertex, while the daughter tracks should have a large impact parameter. The long-track selection uses tracks with hits in the VELO and the tracking stations (TT and T1-T3). The selection is based on the impact parameters of the K_s and their daughters using the reconstructed primary vertex.

The signal yield in each (p_T, y) bin was extracted using a χ^2 fit to the invariant $m_{\pi\pi}$ of the two tracks mass with a linear function to describe the background and the sum of two gaussian functions to describe the signal yield. To account for K_s produced from collisions with the beam and remaining gas, a beam-gas subtraction was made. More details are given in [2]. The fitted mass distributions for the downstream-track and long-track analysis for the full p_T and y range are shown in Fig. 2 and Fig.3.

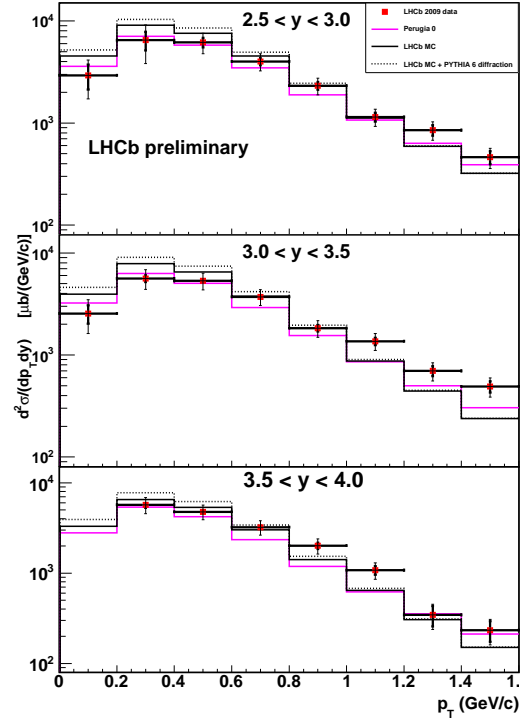


Figure 4: Differential K_s production cross section at $\sqrt{s} = 900$ GeV as function of p_T in different bins of the rapidity. The thick error bars correspond to the statistical, the thin error bars to the total uncertainties. The histograms are different tunings of the PYTHIA generator (see text).

3.4. Results

The cross sections are calculated from both the downstream-track and the long-track analysis. Both lead to consistent results in each phase space bin. But as the two approaches are not statistically independent and the downstream-track analysis has the better statistical power the final results are taken from the downstream-track analysis (except the two lowest p_T bins) in Fig. 2. The differential cross sections are shown in Fig. 4 as a function of the transverse momentum p_T for three different rapidity ranges. They are compared to Monte Carlo predictions using PYTHIA 6.4 with three different tunings [3]:

- the standard settings used by LHCb, including soft diffraction (black dashed line)
- the standard LHCb settings, excluding diffractive events (black solid line)
- the so-called Perugia 0 settings, not including any diffraction (pink line) [4]

Dominating systematic uncertainties of the measurement are systematics on the determination of the luminosity ($\sim 15\%$), the agreement between data and

Monte Carlo for the efficiency determination ($\sim 10\%$), the fit stability ($\sim 4\%$) and the stability of the selection cuts ($\sim 4\%$).

4. $\frac{\bar{\Lambda}}{\Lambda}$ production ratio measurement

A preliminary measurement of the $\frac{\bar{\Lambda}}{\Lambda}$ production ratio was performed with data recorded in 2010. The analysis was performed at the center of mass energies $\sqrt{s} = 900$ GeV and $\sqrt{s} = 7$ TeV using data samples with an integrated luminosity $L = 0.31$ nb $^{-1}$ and $L = 0.2$ nb $^{-1}$ respectively. All subdetectors were in operation. For the lower energy point the VELO halves were, as in 2009, retracted from their nominal position, this time by 10 mm.

Data samples with two different magnetic field polarizations (upward and downward polarization) were combined for this measurement and compared with each other for systematic checks.

4.1. Event selection

The Λ and $\bar{\Lambda}$ are reconstructed in the modes $\Lambda \rightarrow p\pi^-$ and $\bar{\Lambda} \rightarrow p^-\pi^+$. In the selection the Λ candidates are identified by building the invariant mass of two oppositely charged track. Only tracks with hits in the VELO and the tracking stations (TT and T1-T3) were used. The selection requires the Λ or $\bar{\Lambda}$ to point back to the primary vertex to minimize the fraction of particles produced in material interactions. In addition cuts on the track quality and the impact parameter were applied.

4.2. Results

The results of the measurement are shown in Fig.5 for $\sqrt{s} = 900$ GeV and in Fig. 6 for 7 TeV. They are compared with Monte Carlo predictions using two different PYTHIA 6.4 settings: the standard LHCb settings (black line) and the Perugia 0 settings (pink line). A preliminary examination of the systematic uncertainties leads to a 2% relative and additional 0.02 absolute uncertainty, where the dominant parts are uncertainties of matching the Monte Carlo p_T distribution to data and the uncertainty of the material interaction cross section for particle and antiparticle. Both the results for $\sqrt{s} = 900$ GeV and $\sqrt{s} = 7$ TeV are also displayed in Fig. 7 as a function of the difference of the beam rapidity and the rapidity of the reconstructed Λ : $\Delta y = y(\text{beam}) - y(\Lambda)$. This allows a direct comparison of data taken at different energies. In addition a measurement of the STAR collaboration is shown (green).

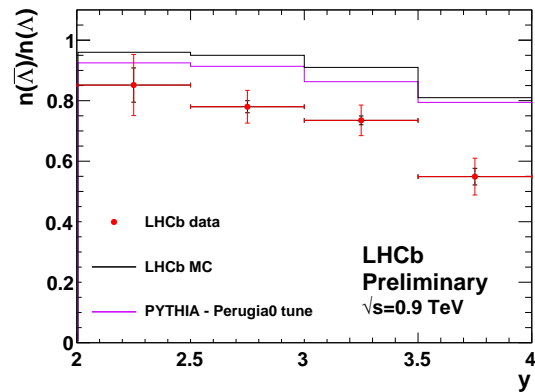


Figure 5: $\frac{\bar{\Lambda}}{\Lambda}$ production cross section at a center of mass energy of $\sqrt{s} = 900$ GeV as a function of the rapidity y . The error bars show the total uncertainty. The histograms show different Monte Carlo models (see text).

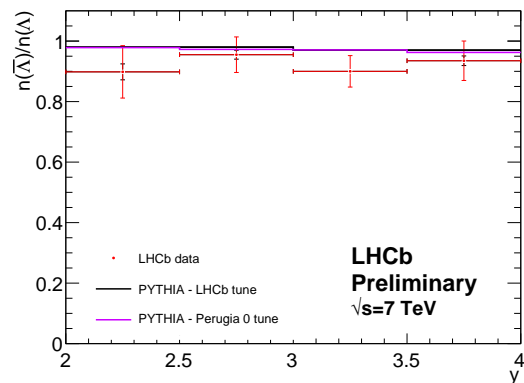


Figure 6: $\frac{\bar{\Lambda}}{\Lambda}$ production ratio at a center of mass energy of $\sqrt{s} = 7$ TeV as a function of the rapidity y . The error bars show the total uncertainty. The histograms show different Monte Carlo models (see text).

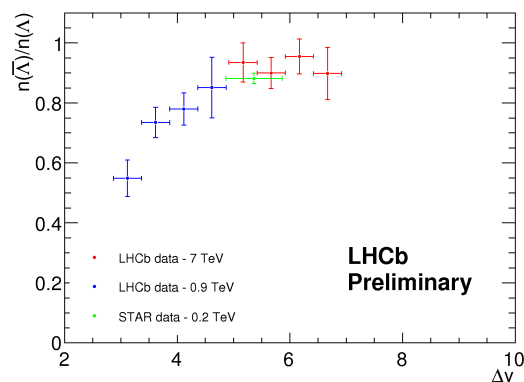


Figure 7: $\frac{\bar{\Lambda}}{\Lambda}$ production ratio at center of mass energy of $\sqrt{s} = 7$ TeV and $\sqrt{s} = 900$ GeV as a function of the difference between beam and Λ rapidity (see text).

5. Conclusion

Using the first data collected in 2009 and 2010 the LHCb detector has been shown to perform well. All subdetectors already exhibit performances very close to their nominal values. Due to the unique angular coverage in forward direction LHCb has, in addition to its flavour-physics program, also a good opportunity to measure interesting forward minimum bias physics. Studies of a K_s differential production cross section measurement at a center of mass energy $\sqrt{s} = 900$ GeV were presented. The results show reasonable consistency with expectations based on the PYTHIA Monte Carlo generator. In addition a preliminary study of the $\frac{\Lambda}{\bar{\Lambda}}$ production ratio was performed. The results for $\sqrt{s} = 900$ GeV show small differences from the generator predictions. The integrated luminosity of $L = 1 \text{ fb}^{-1}$ expected in

2011 will also allow LHCb to perform the planned flavour-physics measurements with the potential to discover New Physics effects.

References

- 1 The LHCb Collaboration, "The LHCb Detector at LHC", JINST 3 (2008) S08005.
- 2 The LHCb Collaboration, "Prompt K_s^0 production in pp collisions at $\sqrt{s} = 900\text{GeV}$ ", Physics Letters B 693 (2010) pp. 69-80
- 3 T. Sjöstrand, S.Mrenna and P.Skands, "PYTHIA 6.4 physics and manual", JHEP 05 (2006) 026.
- 4 P.Z.Skands, "The Perugia tunes", CERN-PH-TH-2010-113, arXiv:1005.3457v1 [hep-ph], May 2010